Mono-axial Solar Tracker with Equatorial Mount, for an improved Model of a Photovoltaic Panel

Hicham Bouzakri*‡, Ahmed Abbou**

*Department of Electrical Engineering, Mohammadia School of Engineers, Mohamed V University in Rabat, Morocco,

**Department of Electrical Engineering, Mohammadia School of Engineers, Mohamed V University in Rabat, Morocco,

(hicham1516@yahoo.fr, abbou@emi.ac.ma)

‡Corresponding Author; Hicham Bouzakri, NR 114 Street H Subdivision El Wafae, Khemisset, Tel: +212641652332,

Hicham1516@yahoo.fr

Received: 12.03.2020 Accepted:15.04.2020

Abstract- In order to maximize the efficiency of a photovoltaic panel, a mechanical system known as a solar tracker is introduced. This paper offers a model of a solar tracker that allows the photovoltaic panel with a single tracking axis and a single motor to receive a quantity of solar radiation similar to those received by a normal surface. Which will reduce the cost of production, facilitate maintenance and minimize the consumption of the system, keeping the maximum performance throughout the year. Our solar tracker uses a modified equatorial mount, in order to follow the sun perfectly. Theoretical studies show that the yield of such a device varies according to the seasons between 91.7% at the winter and summer solstice, and 100% at the equinoxes compared to a normal surface to solar radiation. In order to compensate the loss at the solstices, we proposed to introduce mirrors at the top and bottom of the photovoltaic panel of a well-calculated size and angle. After carrying out the project, a real comparison made, showed us that our model offers an efficiency of about 43.46% compared to a fixed installation of the photovoltaic panel.

Keywords solar tracker, photovoltaic panel, mono axial, Sun tracking, equatorial mount, radiation.

1. Introduction

Morocco has embarked for almost a decade on an ambitious program to strengthen renewable energies, which are too largely dependent on fossil fuels.

Photovoltaic energy is one of the renewable energies in which policies are more and more interested. It has taken an important place in the field of production. This energy sector is based on the direct conversion of solar radiation into electricity [1].

In order to maximize the production of a photovoltaic panel and absorb the maximum of solar radiation, we added a so-called solar tracker system that orient itself to direct solar radiation and therefore follow the movement of the sun from sunrise to sunset.

According to theoretical and practical studies, there are two types of solar trackers: a single-axis solar tracker [2,3,4,5,6] and a two-axis solar tracker [7,8,9].

A two-axis solar tracker makes possible to follow the sun more precisely that the single axis and have more performance. However, using a single-axis system reduces the cost of production and maintenance.

In order to maximize the efficiency of a fixed photovoltaic panel, the panel must face the south and tilt at an angle equal to the attitude of the place [10]. Any comparison of the performance of solar trackers is done with a fixed installation.

A study done by researchers in Morocco With a two-axis solar tracker shows an increase of 32% Compared to a fixed system [11]. This prototype uses a CCD camera to locate the position of the sun and two "DiseqC motor" type motorization systems, which implies an increase in production cost.

In the same vein, another Comparative study in Bangladesh of three types of solar tracking systems; a fixed system, a single-axis tracker and a double-axis tracker; shows that with a single-axis system, they have an increase in efficiency from 25% to 40% compared to a fixed system, while with a duel-axis system an increase between 26% and 45% compared to a fixed system [12]. According the results the difference between the two systems is negligible, thus they concluded

that a mono-axial tracking system would be an economical option for their site.

Another experimental work was done by a researcher in Jordan on four electromechanical solar tracking systems: two axes, a vertical axis, an east-west axis and a north-south axis. The results showed increases in electrical power gain up to 43.87%, 37.53%, 34.43% and 15.69% for the two axes, followed by east-west, vertical and north-south, respectively. , compared to a fixed surface [13].

In addition, another comparative study was carried out by researchers in Kazakhstan where they proposed a prototype for solar tracking with two axes, horizontal and vertical, and the results showed that the dual-axis system produced 31.3% more power compared to the fixed photovoltaic module [14].

Similarly, a researcher in Turkey deployed a two-axis horizontal and vertical tracking system capable of determining by pre-calculated formulas the angle of azimuth and altitude over a period of one year. The prototype produced 42.6% more energy than a fixed system [15]. Since it uses an open loop system (no solar collector) this type of tracker will continue to follow the sun despite an overcast sky, which causes a loss of energy and risks having a total discharge of the batteries.

All the previous research focuses mostly on production and neglects some essential indicators for system recovery, such as the cost of production and the energy dissipated during the follow-up mode.

This paper proposed a solar tracker concept based on the equatorial mount, as well as a model added to the photovoltaic panel. It will maximize the reception of solar radiations (similar to a normal surface to solar radiation) during the day and throughout the year with a single monitoring axis, in order to reduce the cost of production, facilitate maintenance and minimize system consumption while keeping performance to the maximum.

Our study is based on three major pillars. Foremost, an explanation of the mono-axial equatorial mount proposed for our solar tracker. Then a theoretical study which shows that our equatorial system receives almost the same amount of solar irradiation during periods close to the equinoxes as that of a surface normal to solar radiation, and decrease up to 91.7% for a period close to the solstices (summer solstice and winter solstice).

we approach in a third place a geometric study based on a reflection, that will allow the system to compensate for the loss of solar irradiation during the periods of solstices, by adding mirrors at the top and bottom of the panel, thus keeping the efficiency of our concept almost to the maximum throughout the year. After having completed the system, our study will be closed with experimental results.

2. The Equatorial Mount Proposed for The Solar Tracker

Most solar trackers have used a tracking model based on two axes, horizontal and vertical. In this case, it is necessary to vary the two axes (via two motors), in order to follow the sun perfectly “Fig.1”.

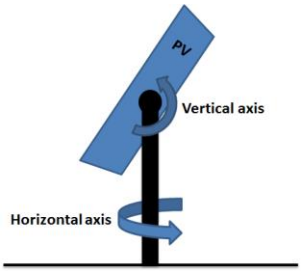

Figure 1. Two-axis solar tracker.

Our paper proposes the use of an equatorial mount modifier, allowing the photovoltaic panel to easily and specifically follow the sun with a single axis.

On Earth, all the astronomical objects in the sky (sun, moon, planets, stars, galaxies, nebulae, etc.) seem to be moving from east to west (day and night). This movement is due to the fact that the earth turns on itself on a north-south axis of rotation. All the astronomical objects including the sun do an apparent circular path around the polar star (Polaris), since it is almost on the axis of Earth's rotation“Fig.2” “Fig.3”. In order to be able to follow these objects perfectly, it suffices to orient the tracking axis towards the polar star “Fig.4” [16].

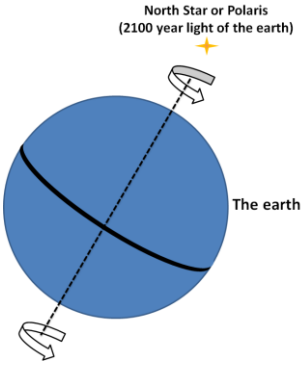

Figure 2. The position of the polar star with respect to the axis of rotation.

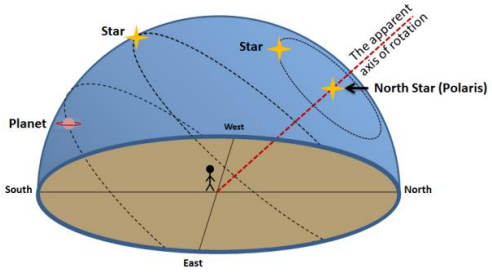

Figure 3. The apparent path of celestial objects.

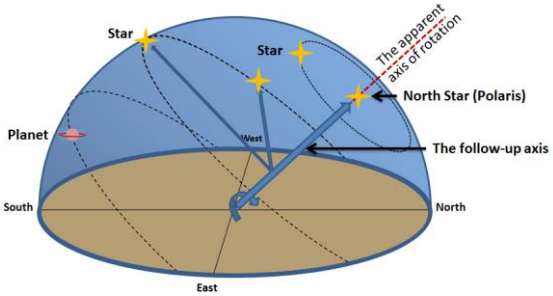

Figure 4. The orientation of the follow-up axis.

The equatorial mount uses this principle to precisely follow the sky's astronomical objects via a single axis. This mount is widely used for astronomical telescopes [16].
The goal of our work is to make a solar tracker model using this principle in order to be able to follow the sun perfectly with a single motor.
We all know that the earth's axis of rotation is tilted at an angle equal to 23.45 ° "Fig.5", while the earth rotates around itself in 24 hours and at the same time makes a revolution of 365.25 days around the sun. This implies the change in the apparent solar path during the year and therefore the seasonal change "Fig.6".

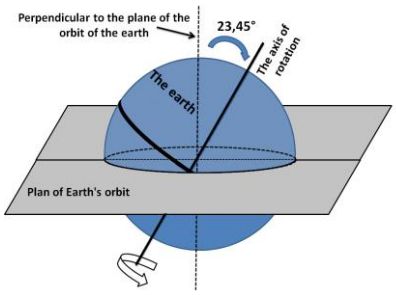

Figure 5. Representation of the equator, northern tropics and southern tropics.

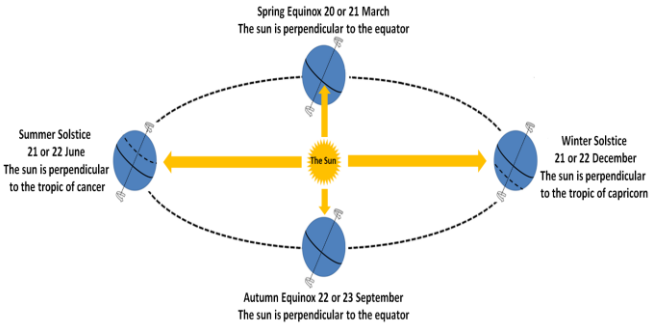

Figure 6. Movement of the earth around the sun.

The apparent solar path remains of course circular around the North Star, but it deviates every day until it reaches an angle of 23.45 ° (+ 23.45 °) at the top of the celestial equator and 23.45 ° (-23.45 °) above. This is the solar declination angle "Fig.7". [17]

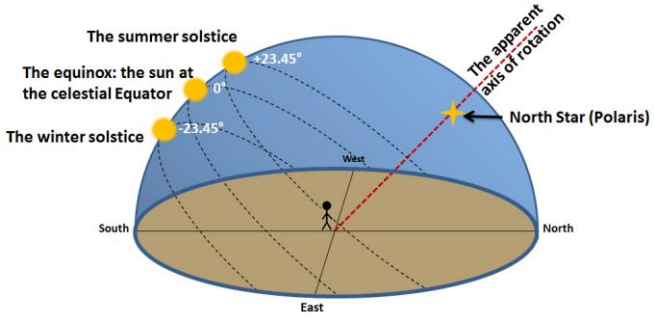

Figure 7. The angle of solar declination.

It is calculated by the following relation: [17]

$$\delta = 23.45 \sin\left[\frac{360}{365}(d_n + 284)\right] \text{ in degrees} \quad (1)$$

With d_n Day number of the year, 1 corresponds to January 1 and 365 to December 31.

We proposed to put the photovoltaic panel on the tracking axis, so as to orient itself towards the celestial equator. Therefore, this one will be perfectly perpendicular to the solar radiation during the equinox days (March 21 and September 23) or the sun will be on the celestial equator "Fig.8". Beyond the equinoxes the solar radiation touches the panel with an equal inclination to the absolute value of the solar tilt. On solstice days (summer solstice on June 21 and winter solstice on December 23), the sun's rays will be at maximum deviation from the solar panel (23.45 °) "Fig.8".

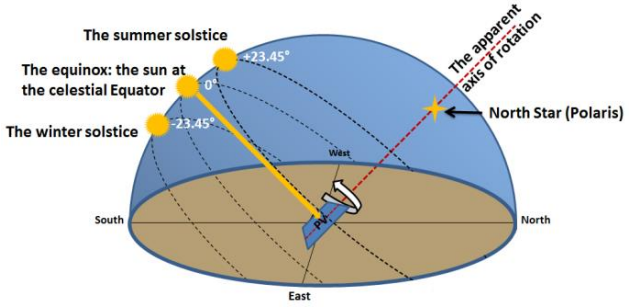

Figure 8. The receiving surface is oriented perpendicular to the celestial equator (the solar tracking axis is oriented towards the polar).

In the next chapter, we will compare the amount of solar irradiation absorbed by a surface mounted on our model and that normal to solar radiation (a surface always oriented towards the sun), in order to draw a graph which shows in detail the annual variation of this quantity compared to the maximum.

3. The Theoretical Comparison

In order to theoretically enhance our proposed model, we will make a comparison between the amount of solar irradiation absorbed by a surface mounted on our model and the quantity of solar irradiation absorbed by a surface normal to solar radiation.

3.1 The amount of solar irradiation from a surface normal to solar Radiation

A surface normal to solar irradiation is a surface constantly oriented perpendicular to direct solar rays. So it receives the maximum irradiation that a surface can receive "Fig.9". [17]

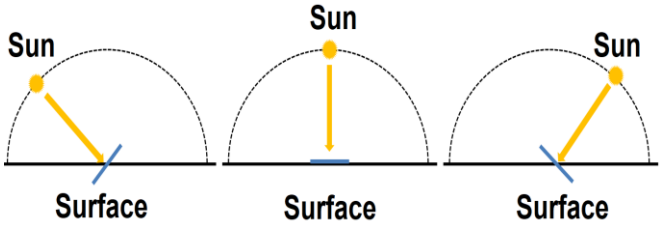

Figure 9. Normal surface to solar rays.

We know that the solar irradiation is attenuated during its passage through the Earth's atmosphere, and since this reduction will be identical for the two comparison systems, we will make the theoretical calculations outside the atmosphere.

The extraterrestrial irradiance on a normal surface to the solar rays is [17]:

$$\dot{I}_{on} = \dot{I}_{SC}(r_0/r)^2 = \dot{I}_{SC}E_0 \quad (2)$$

With:

r Actual sun-earth distance (AU).

r_0 Mean sun-earth distance, 1 AU.

$\dot{I}_{SC}$ The solar constant $\dot{I}_{SC} = 1353\ W\ m^{-2}$.

E_0 Eccentricity correction factor of earth$(r_0/r)^2$.

$\dot{I}_{on}$ Is the maximum amount of solar radiation that a surface can receive.

3.2 The amount of solar irradiation from an inclined surface oriented towards the celestial equator

The amount of solar irradiation outside the atmosphere of an inclined surface oriented towards the celestial equator is [17]:

$$\dot{I}_{o\beta} = \dot{I}_{SC}E_0 = \dot{I}_{on}\cos(\theta_0) \quad (3)$$

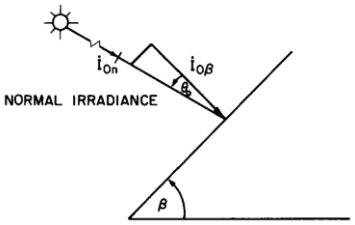

Figure 10. Irradiance on inclined plane tilted toward the equator [17].

Since we fixed the photovoltaic panel on our solar tracker so as to orient itself towards the celestial equator, the direct solar radiation will be perpendicular to the photovoltaic panel during the days of equinox where the sun is on the celestial equator "Fig.11". When the sun leaves the celestial equator towards the summer or winter solstice, its direct radiation will be tilted to the photovoltaic panel at an angle equal to the solar tilt "Fig.12" "Fig.13".

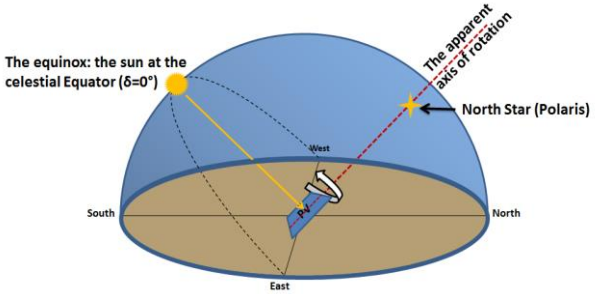

Figure 11. The position of the panel relative to the sun during the equinox.

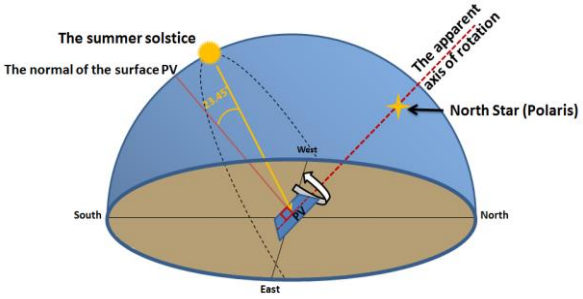

Figure 12. The position of the panel relative to the sun during the summer solstice.

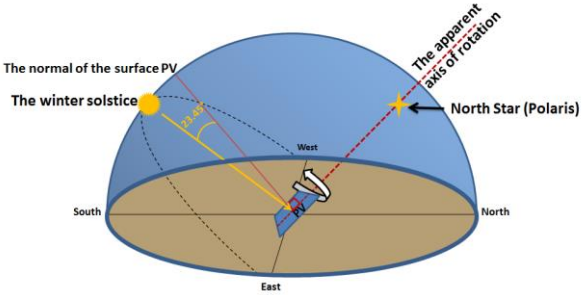

Figure 13. The position of the panel relative to the sun during the winter solstice.

On the summer solstice day (June 21) or the winter solstice day (December 23), we will have:

$$\dot{I}_{o\beta} = \dot{I}_{on}\cos(\pm 23.45°) = 91.7\%\dot{I}_{on} \quad (4)$$

That is to say that the amount of solar irradiation outside the atmosphere of a surface mounted on our solar tracker varies between 91.7% and 100% compared to the maximum amount of irradiation. The graph below shows the annual variation of the amount of solar irradiation outside the atmosphere compared to the maximum (the amount received by a surface normal to solar radiation) "Fig.14".

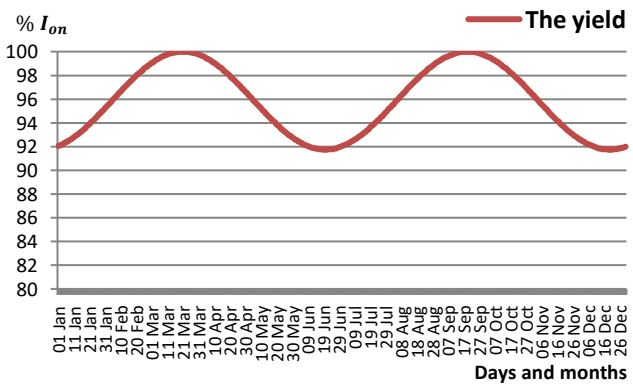

Figure 14. The annual solar irradiation outside the atmosphere received by a surface mounted at our tracking system.

4. The Proposed Modification to The Photovoltaic Panel

In order to compensate the solar irradiation decrease during the solstice days (winter solstice and summer solstice), we will introduce to the photovoltaic panel a reflection system based on the addition of the two mirrors at the top and bottom. The top one reflects the quantity lost during the summer solstice (100% -91.7%=8.3%), and the bottom one reflects the quantity lost during the winter solstice (8.3%) "Fig.15".

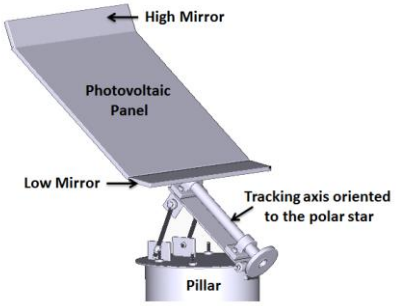

Figure 15. The photovoltaic panel with both mirrors up and down on our equatorial solar tracker.

During the equinox, the two mirrors must have no influence on the photovoltaic panel since it is perpendicular to the solar radiation "Fig.16". Gradually, as trajectory of the sun move to the winter solstice, the bottom mirror reflects the rays towards the panel, the top one has no influence "Fig.17". Likewise for the summer solstice the upper mirror reflects towards the panel and the lower one has no influence "Fig.18". The mirror size is calculated to just compensate for the loss due to the solar inclination (+23.45 ° at the summer solstice and –23.45 ° at the winter solstice) which is equal to 8.3 %.

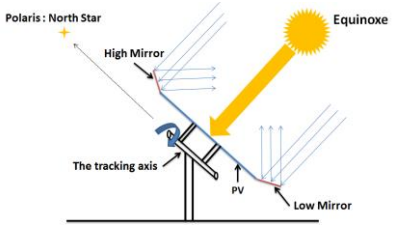

Figure 16. The two mirrors added at the top and bottom
will have no influence on the photovoltaic panel during the days of the equinoxes.

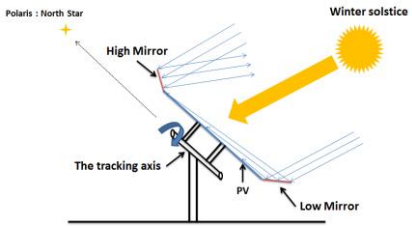

Figure 17. The mirror influence adds to the photovoltaic panel at the bottom, to offset the decreasing
in yield during the winter solstice.

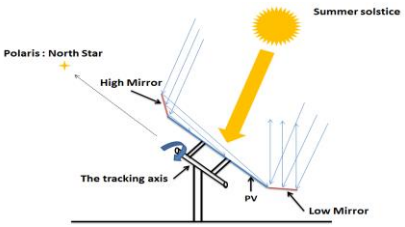

Figure 18. The mirror influence adds to the photovoltaic panel at the top, to compensate for the decrease in yield during the summer solstice.

In this way, the yield of the photovoltaic panel is kept almost at the maximum throughout the year, with a single tracking axis.

The width calculation and the angle of inclination of each mirror:

During the summer or winter solstice, the surface of each mirror must reflect 8.3% of the amount of direct solar irradiation absorbed by our photovoltaic panel, in this way, it receives the maximum that a normal surface receives to solar radiation. This quantity is represented by the surface ABCD and it will be reflected by the EFJH mirror towards the panel "Fig.19". Therefore, the surface ABCD must represent 8.3% of the FIGJ surface (the surface of the photovoltaic panel) "Fig.19".

So: $$AB \times BC = 0{,}083 \times FI \times IG \quad (5)$$

Since the length of the added mirror is equal to that of our photovoltaic panel "Fig.19": AD=BC=EH=FJ=IG

So "Eq.(5)" becomes: $$AB = 0.083 \times FI \quad (6)$$

The goal is to calculate the width of the FE mirror and the angle of inclination of that mirror from the photovoltaic panel.

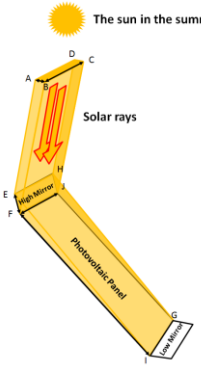

Figure 19. The amount of solar radiation reflected by the high mirror towards the photovoltaic panel.

At summer solstice, the solar rays touch the panel with an inclination equal to the solar inclination $\delta = +23.45°$ with respect to the normal of the surface of the panel "Fig.20".

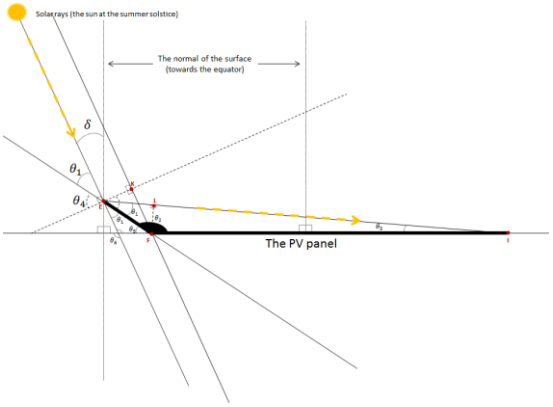

Figure 20. The mirror installed to photovoltaic panel destined for summer solstice.

To add 8.3% the radiation lost on the summer solstice day, the quantity reflected by the mirror (presented by EK) must be 8.3% of the surface of our panel (presented by FI) "Fig.21".

And we have "Fig.19" "Fig.20": AB= EK

So the "Eq. (6)" becomes: $EK = 0{,}083 \times FI$ (7)

Knowing that a mirror does not reflect the totality of received radiation. The mirror reflection factor used (R) must be taken into consideration.

So the "Eq. (7)" becomes: $\frac{EK}{FI} = \frac{0{,}083}{R}$ (8)

The goal is to calculate the angle of inclination of mirror θ_5 with respect to the panel and its length EF.

And we have "Fig.20": $\sin(\theta_3) = \frac{FL}{FI}$ (9)

$$\sin(\theta_1) = \frac{FL}{FE} \quad (10)$$

So "Eq. (9)" becomes: $\sin(\theta_3) = \frac{FE}{FI} \times \sin(\theta_1)$ (11)

Also we have: $\cos(\theta_4) = \frac{EK}{FE}$ (12)

So: $FE = \frac{EK}{\cos(\theta_4)}$ (13)

So "Eq.(11)" becomes: $\sin(\theta_3) = \frac{EK}{FI} \times \frac{\sin(\theta_1)}{\cos(\theta_4)}$ (14)

And we have "Fig.20": $\theta_4 = 90° - \theta_1$

So "Eq. (14)" becomes:

$$\sin(\theta_3) = \frac{EK}{FI} \times \frac{\sin(\theta_1)}{\cos(90°-\theta_1)} = \frac{EK}{FI} \quad (15)$$

With "Eq. (8)" equation (15) becomes:

$$\sin(\theta_3) = \frac{0{,}083}{R} \quad (16)$$

Also we have "Fig.20":

$$\theta_1 + \theta_2 + \theta_3 = 180° \quad (17)$$

$$\theta_1 + \theta_5 + \theta_6 = 180° \quad (18)$$

$$\theta_5 + \theta_2 = 180° \quad (19)$$

$$\delta + \theta_1 + \theta_5 + 90° = 23{,}45° + \theta_1 + \theta_5 + 90° = 180°$$

So: $\theta_1 + \theta_5 = 66.55°$ (20)

If we take R = 1 (a total reflection of radiation) then according to "Eq. (16)" we will have:

$$\sin(\theta_3) = 0.083 \quad \text{So:} \quad \theta_3 = 4.76°$$

According to "Eq. (17)", "Eq. (18)", "Eq. (19)" and "Eq. (20)" we will have:

$$\theta_1 = 30.9° \quad ; \quad \theta_2 = 144.34° \quad ; \quad \theta_5 = 35.65°$$

Finally and according to "Eq. (11)" we will have:

$$FE = 0{,}16 \times FI \quad (21)$$

Thus, the width of the mirror must be calculated from the languor of the panel used according to "Eq. (21)" and the angle of inclination will be $\theta_5 = 35.63°$.

Note:

- Those calculations are valid with a mirror reflection ratio R = 1. If we change R the Results change. And also one must take into consideration the reflection rate of glass that covers the solar panel cells.
- At the summer solstice just the mirror at the top that reflects the light towards the panel. The one in the bottom which is intended for the winter solstice, reflected light away from solar panel "Fig.18".

5. The Annual Radiation Received by Our System

With the equatorial mount without the top and bottom mirrors, the solar radiation outside the atmosphere received is between 91.7% and 100% "Fig.14".

The addition of a reflection system compensated for the loss of radiation during the solstice days. However, we have to calculate the added radiation between the solstices and the equinoxes. To do this, we must first know the angle from which the top or bottom mirror does not reflect direct sunlight towards our panel "Fig.21".

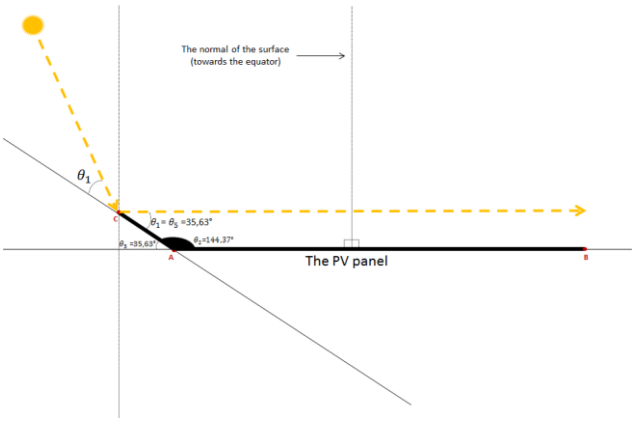

Figure 21. The angle from which the mirror at the top does not reflect light towards the solar panel.

The angle from which the top mirror (dedicated to the summer solstice) does not reflect light towards the solar panel is:

$\theta_1 = \theta_5 = 35.63°$ (The reflected radiation is parallel to the panel "Fig.21").

So we have to calculate the added amount of solar radiation between $\theta_1 = 30.87°$ and $\theta_1 = 35.63°$ "Fig.22".

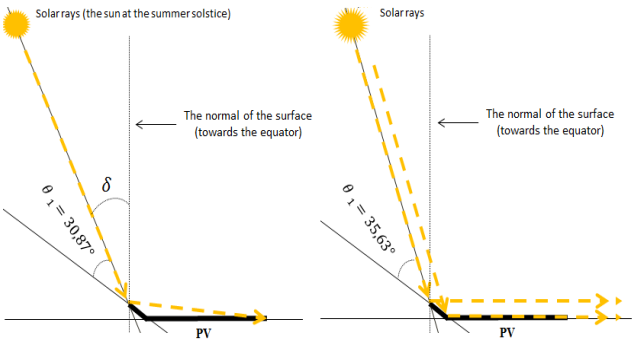

Figure 22. The solar rays that touch the mirror between $\theta_1 = 30.87°$ and $\theta_1 = 35.63°$.

At $30.87° < \theta_1 < 35.63°$ the light touches part of our solar panel, so we have to calculate just what is reflected on the solar panel "Fig.23".

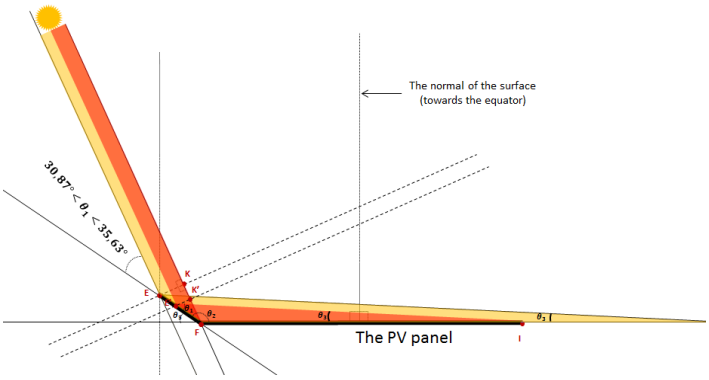

Figure 23. The reflection of the solar radiation from the mirror when θ_1 between 30.87 ° and 35.63 °.

The quantity of reflected light represented by EK distributed on a surface represented by FI' "Fig.23", the goal is to calculate the quantity which just touches the panel represented by FI compared to the reflected quantity E'K' (represented by the red color in "Fig.23".
With "Eq. (15)" and the "Fig.23" we will also have:

$$\sin(\theta_3) = \frac{EK}{FI'} = \frac{E'K'}{FI} \quad (22)$$

And we have $\theta_3 = 180° - \theta_2 - \theta_1$ (23)

And we have: $\theta_2 = 144.37°$ (It does not change, already calculated before)

So the "Eq.(22)" becomes:

$$\sin(35.63° - \theta_1) = \frac{E'K'}{FI'} \quad (24)$$

At the summer solstice $\theta_1 = 30.87°$ we have $\frac{E'K'}{FI'} = 8.29\%$ If $\theta_1 = 35.63°$ so $\frac{E'K'}{FI'} = 0\%$ this is the case of the reflected light does not touch the solar panel "Fig.22".

5.1 the summer solstice

We can calculate θ_1 compared to δ as the sun enters the equinox and the summer solstice "Fig.22":

$$\theta_1 = 30.87° + (23.45° - \delta) = 54.32° - \delta \quad (25)$$

So if $30.87° < \theta_1 < 35.63°$

we'll have : $+23.45° < \delta < +18.69°$

According to "Eq. (1)":

- The day or the angle of solar inclination equal $\delta = +23.45°$ is d≈172 (the summer solstice 21 June).
- The days or the angle of solar inclination equal $\delta = +18.69°$ are d≈135 (15 May) and d≈210 (29 July) (the sun passes twice through $\delta = +18.69°$).
- The graph below shows the annual amount of solar radiation added to the panel by the top mirror (The yield is calculated by "Eq. (24)" between d=135 and d=210) "Fig.24".

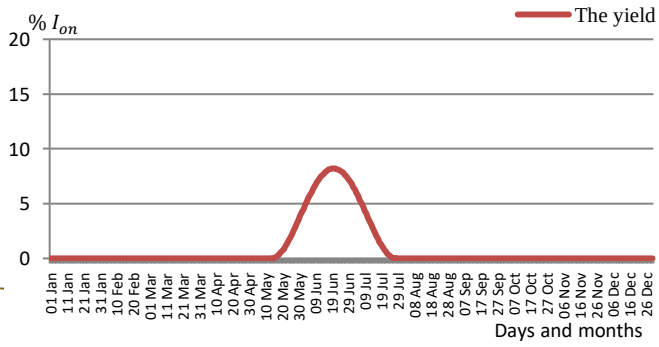

Figure 24. The annual amount of solar radiation added to the panel by the top mirror.

5.2 The winter solstice

During the winter solstice the mirror at the bottom which must reflect the amount of 8.3% of solar radiation.

And since the solar angle of inclination between the equinox and the winter solstice is: $0° < \delta < -23.45°$

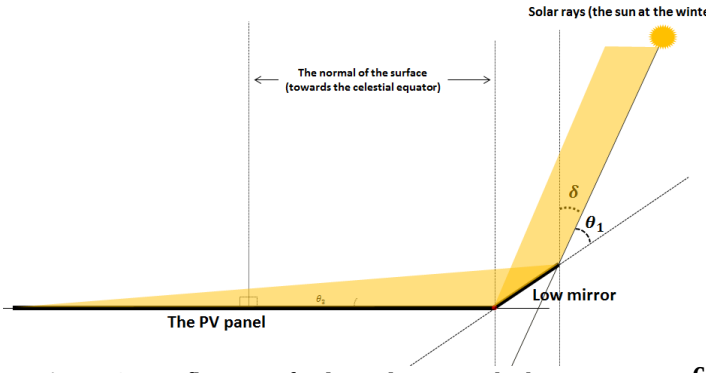

Figure 25. Reflection of solar radiation at the bottom mirror panel.

And we'll have "Fig.25":

$$\theta_1 = 30.87° + (23.45° + \delta) = 54.32° + \delta \quad (26)$$

So if $30.87° < \theta_1 < 35.63°$

we'll have: $-18.69 < \delta < -23.45°$

According to "Eq. (1)":

- The day or the angle of solar inclination equal $\delta = -23.45°$ is d≈355 (the winter solstice 21 December).
- The days or the angle of solar inclination equal $\delta = -18.69°$ are d≈27 (27 January) and d≈317 (13 October the sun passes twice through$\delta = -18.69°$).

The graph below shows the annual amount of solar radiation added to the panel by the bottom mirror (The yield is calculated by "Eq. (24)" between d=317 and d=27) "Fig.26".

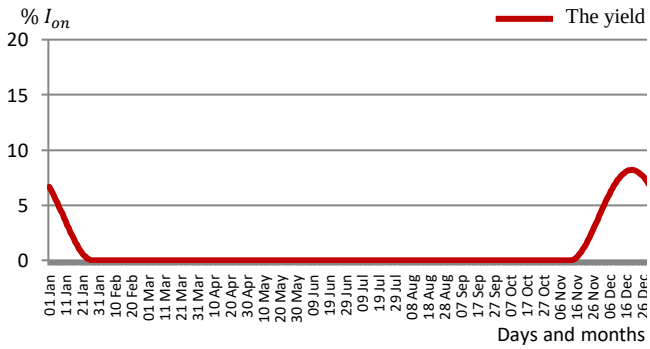

Figure 26. The annual amount of solar radiation added to the panel by the bottom mirror.

Therefore the annual radiation received by our system is represented by the graph above "Fig.27".

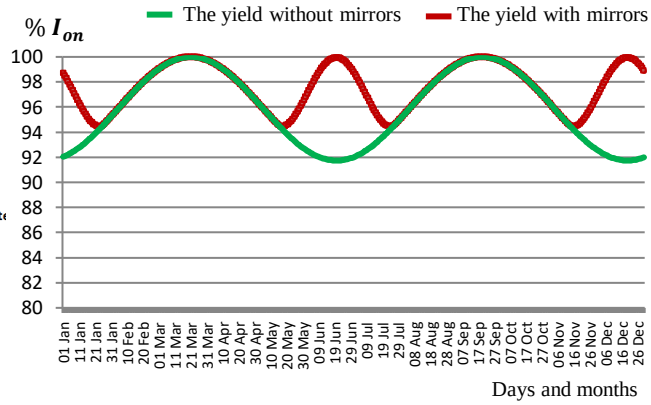

Figure 27. The annual amount of solar radiation added to the panel by the bottom and the top mirror

6. Realization

6.1 The realization of the equatorial mount

As we have seen, an equatorial mount is a mechanism that makes it easier for us to follow the astronomical objects with only one axis; this axis must point towards the North Star (Polaris). To facilitate the setting up of the mount (orientation towards the North Star), we use a round hollow steel tube in order to visualize the North Star during the installation of the system (it is an installation made during the night) "Fig.28". If a solid tube is used, it will be oriented towards the north and will be tilted at an angle equal to the latitude of the place "Fig.29".

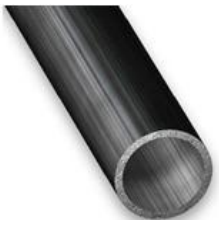

Figure 28. Round and hollow iron tube.

Figure 29. The orientation of the tracking axis towards the pole star.

This axis will be held by two bearings, and the shaft is held in position by two setscrews on the inner ring of each bearing "Fig.30".
The base is intended to support the frame with the solar panels. It will be securely attached to a concrete block "Fig.30". In order to take the measurements and do the test we will fix it on a tripod "Fig.31".
The base consists of a rectangular base of 250 x 90 mm, linked with a flat iron of the same size via a bolt screw of 120 mm in length, to give access to the variation of the angle between the two irons dishes. This angle is that of latitude of the place "Fig.30" "Fig.31".

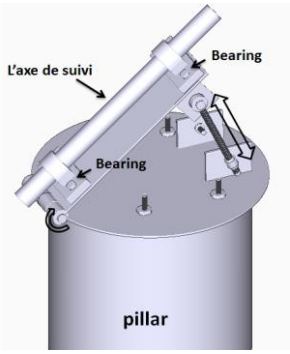

Figure 30. The structure of the equatorial mount to be produced.

Figure 31. The equatorial mount on a tripod.

6.2 The motorization

In order to support a set of solar panels, we will use a worm wheel type reducer "Fig.32".

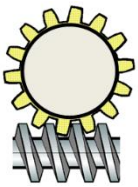

Figure 32. Worm gear reducer.

For our prototype, we will use a "DiseqC motor" type reducer with a reduction ratio equal to 1/6000.
In order to minimize the consumption and increase precision, we have chosen to use a unipolar stepper motor.

- *The size of motor and its power*

  Unipolar stepper motor 55SI-25DAYA, with the following characteristics:
  Nominal Rated Input Voltage: 12 Volts.
  Rated current: 330mA.
  Coil resistance: 36Ohms.
  Inductance: 37mH.
  Degree of step: 7.5°
  Number of steps per revolution: 48.

  Shaft diameter: 6.35mm.
  Motor diameter: 55mm.
  Motor height: 25mm.
  Maximum motor torque (engine blocked): 1350g/cm.

- *The Maximum load*

Because the reducer used at a ratio of 1/6000 and the motor at a blocked torque of 1350g / cm. At the output of the reducer, there will be a maximum torque of the order of: 1350g / cm x 6000 = 8100kg / cm So it's a couple powerful enough to support a set of photovoltaic panels.

Consequently, the rigidity of the structure will limit the number of PV modules installed. The coupler used is of the DiseqC motor type, which is intended to support a maximum of approximately 18kg (example a photovoltaic panel of the CSUN310 60M type with a power of 300w and a dimension of 1640x900x35mm). And since the output of our coupler is reinforced by two bearings, we can probably exceed this limit.

6.3 The solar collector

To simplify the implementation, we will use a solar collector with two LDR (Light Dependent Resistor), since we are using a mono-axial tracking system.

A wall separates the two LDR. If one of them is in the shade, the system will activate the motor on the right or on the left in order to keep the two LDR lit, in this way the solar panel remains constantly oriented to the solar radiation "Fig.33".
The system starts correcting as soon as the shadow of the wall touches one of the two LDR "Fig.33".

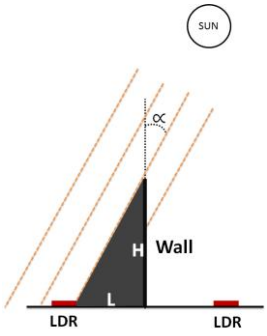

Figure 33. Solar captor with two LDR.

This angle is calculated by the following relationships:

$$\tan \propto = \frac{L}{H} \qquad (27)$$

With:

$\propto$: The angle of the shadow that touches the LDR.
L : The distance that describes the solar shadow on the sensor.
H : The height of the wall.

The angle α decreases, if the height of the wall increases or the distance L decreases. As a result, the sunshade quickly hits the LDR, which causes the correction to work.
A low-energy tracking system, however, is to take an ideal angle so that the correction does not occur for a very short time.
We opted for a correction every 5 min. That is to say that after 5 min of the direct orientation of the sensor towards the sun, the shadow touches one of the LDR and the control card detects the decrease in its resistivity, which causes the operation of the correction established by the engine.
To calculate the suitable angle at 5 min, just apply the rule of three. Take 12 hours = 720 min as an average between sunrise and sunset, that is, a 180 ° course:

$$\propto = \frac{5\ \text{min} \times 180°}{720\ \text{min}} = 1.25° \quad (720\ \text{min} = 12\text{h x } 60\ \text{min})$$

So with "Eq. (27)" we have: $\tan(1.25°) = \frac{L}{H} = 0.02182$

So: L=0.02182H

If we choose a height of = 60 mm, the distance is therefore = 1.3 mm.

6.4 The control card

The control card is the card that allows the system to control the tracking of the mount. It is based on the PIC16F876 microcontroller.
The two analog values retrieved from the solar collector will be converted into digital codes through the Analog / Digital inputs of the microcontroller.
Then a comparison made between the two values, in order to know the position of the sun relative to the sensor. If the two values are equal, the system is in standby mode, if one of them is lower than the other the card will activate the motor on the right or on the left, until the equality of the two values "Fig.34".

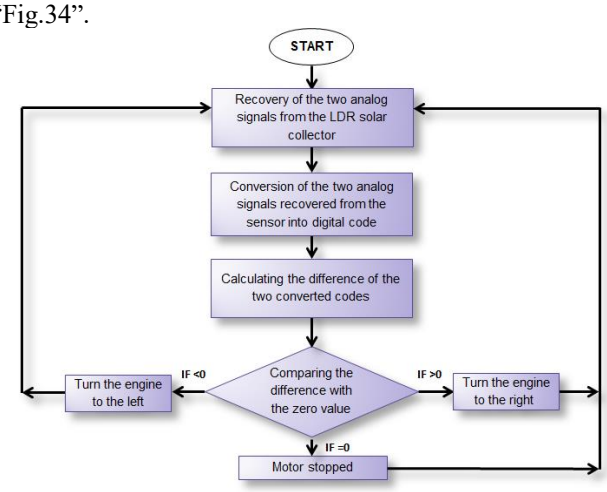

Figure 34. The flowchart of the control board of our solar tracker.

6.5 The bottom and top mirrors

The previous calculations were made with a reflection rate R=1. We actually the mirror does not reflect all of the solar radiation and also the glass that covers the solar cells prevents a significant part of the radiation (by absorption and reflection).

The panel used for the test has a dimension of $63\text{cm} \times 57\text{cm}$ "Fig.35".

Figure 35. The panel used for the test.

If we consider that R=1 and according "Eq. (21)" we must use a dimension mirror: $63\text{cm} \times 9.12\text{cm}$

With an inclination of $\theta_5 = 35.65°$.

And since we ignore the reflection rate of the mirror and also of the glass that covers the solar panel, we will estimate that R=50%.

So if we repeat the calculations with R = 0.5 we will have a dimension of:

With "Eq.16" we have: $\sin(\theta_3) = \frac{0,083}{R} = 0,166$
SO $\theta_3 = 9.55°$

According to "Eq. (17)", "Eq. (18)", "Eq. (19)" and "Eq. (20)" we will have:

$\theta_1 = 28.5°$; $\theta_2 = 141.95°$; $\theta_5 = 38.05°$

Finally and according to "Eq. (11)"

we will have: $FE = 0,35 \times FI$

So the mirror added has a dimension of $63\text{cm} \times 19.95\text{cm}$ and with an inclination of $\theta_5 = 38.05°$ of that mirror from the photovoltaic panel.

7. Test and Results

7.1 The production

On February 9th, 2020, a real test of two solar panels with the same characteristics was realized. The first panel was in a follow-up mode and the 2nd in a fixed mode.
At noon we reversed the panels to ensure symmetry between the two "Fig.36".

The characteristics of the solar panels are:
$V_{co} = 22.1\text{ V}$, $V_{mpp} = 18.2\text{ V}$, $I_{cc} = 2.95\text{ A}$, $I_{mpp} = 2.75\text{ A}$

Figure 36. The solar panel on the left in the tracking mode, the one on the right in the fixed mode.

So the form factor is: $FF = \frac{(V_{mpp} \times I_{mpp})}{(V_{co} \times I_{cc})} = \frac{P_{mpp}}{(V_{co} \times I_{cc})} = 0.76$

So: $P_{mpp=} 0,76 \times (V_{co} \times I_{cc})$ (28)

We measured every 30 min the V_{co} and I_{cc} to calculate the power of each photovoltaic panel with "Eq. (28)".

The obtained results are shown in Table "Table 1." and Graph "Fig.37".

Table 1. Reading data from solar panels.

	The results of the fixed panel			The results of moving panel		
Hour	Vco (V)	Icc (A)	Pmpp (W)	Vco (V)	Icc (A)	Pmpp (W)
08:00	19.65	0.08	1.19	21.12	0.82	13.16
08:30	20	0.41	6.23	21.11	1.82	29.19
09:00	21.12	0.7	11.23	21.13	2.12	34.04
09:30	21.4	0.95	15.45	21.3	2.34	37.87
10:00	21.4	1.34	21.79	21.3	2.48	40.14
10:30	21.2	1.71	27.55	21	2.68	42.77
11:00	21.4	2.07	33.66	21.2	2.89	46.56
11:30	21.3	2.36	38.20	21.1	2.92	46.82
12:00	21.2	2.7	43.50	21.1	3.03	48.58
12:30	20.9	2.94	46.69	20.8	3.11	49.16
13:00	20.9	3.02	47.96	21	3.14	50.11
13:30	20.5	3.1	48.29	20.7	3.19	50.18
14:00	20.4	3.06	47.44	20.8	3.17	50.11
14:30	20.4	2.99	46.35	20.7	3.25	51.12
15:00	20.4	2.83	43.87	20.8	3.23	51.05
15:30	20.5	2.6	40.50	20.8	3.19	50.42
16:00	20.3	2.3	35.48	20.7	3.14	49.39
16:30	20.4	1.92	29.76	20.8	2.98	47.10
17:00	20.5	1.54	23.99	21	2.78	44.36
17:30	20.2	1.08	16.58	20.9	2.46	39.07
18:00	19.9	0.64	9.67	21	1.93	30.80
18:30	18.6	0.19	2.68	20.7	0.83	13.05
19:00	15	0.02	0.228	17.7	0.05	0.67
Total			638.4	Total		915.85

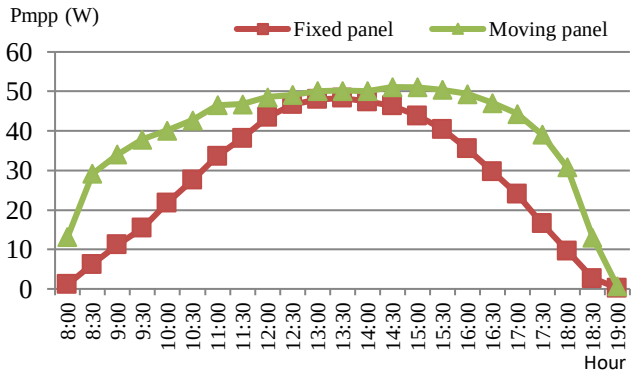

Figure 37. The comparison between a fixed solar panel and that in motion.

Based on the results above, we find an increase of about 43.46% in the solar panel productivity in motion mode compared to fixed mode.

And the test day (February 09, 2020) the two mirrors added to the photovoltaic panel have no influence on the performance "Fig.28".

In order to validate experimentally the effect of its two added mirrors, we did another test on February 15, 2020. This time we programmed the command card so that the follow-up will be instantaneous (instantaneous correction not every 5 min). The choice of February 15, 2020 as the day for carrying out the experiment implies that d=46. For this purpose, the solar inclination on this day will be "Eq. (1)":

$$\delta = 23.45 \sin\left[\frac{360}{365}(46 + 284)\right] = -13.29°$$

Since the bottom mirror reacts to the maximum on our panel on the winter solstice day (-23.45) and the top mirror in the summer solstice day (+ 23.45 °), we will measure the power added to the winter solstice by tilting the photovoltaic panel by: 23.45 ° -13.29 ° = 10.16 ° "Fig.38".

Figure 38. The tilt of the photovoltaic panel for the test of the bottom mirror.

Then we will measure the power supplied by our panel with and without the bottom mirror in order to compare the two results obtained (the tracking correction system is instantaneous).

The table below illustrates the results of the experiment:

Table 2. The results of the second experiment.

The panel without the mirror			The panel with the mirror		
Vco (V)	Icc (A)	Pmpp (W)	Vco (V)	Icc (A)	Pmpp (W)
20.4	3.5	54.62	20.6	3.8	59.49

The results show that the bottom and top mirrors add about 8.91% power to our photovoltaic panel during summer or winter solstice days.

7.2 The consumption

In order to really measure the power consumed by the system, we opted for a real test with a digital multimeter, we measured the voltage and the current of each system block:

- The control card with the solar collector.
- The stepping motor.

Then we calculate the power consumed by the system in stop mode and in follow-up mode.

During the shutdown of the correction system, the measured current of the control card operating at 5 V is 91 mA, while the current flowing through the motor is zero.

So, the power consumed is:

$$P = U \times I = 5V \times 0.091A = 0.4455\ W$$

During the correction, the measured current of the control card which operates at 5 V is 125 mA, and the current flowing through the motor is 150 mA.

So, the power consumed during the correction is:

$$\begin{aligned} \mathrm{P} &= \mathrm{P}_{\textbf{control card}} + \mathrm{P}_{\mathrm{motor}} \\ &= (5\mathrm{V} \times 0.125\mathrm{A}) + (12\mathrm{V} \times 0.15\mathrm{A}) \\ &= 2.425\ \mathrm{W} \end{aligned}$$

During one hour of follow-up, the system must make a journey of 15 ° (360 ° / 24h). Since the sensor has been configured to make the correction every 5 min, the system will be in stop mode for 5 min, then it will start a correction of 1.25 ° (15 ° / (60 ÷ 5)). According to real measurements, this correction lasts on average 10 seconds. So for an hour, the system runs almost 90 seconds and stops 58min and 30 seconds (3510s) (measured results).

In other words, the hourly consumption during monitoring will be:

$$\mathrm{P_h} = \mathrm{P_{stopped}} + \mathrm{P_{correction}}$$

$$\mathrm{P_h} = \frac{(0.455\mathrm{w} \times 3510\mathrm{s})}{3600\mathrm{s}} + \frac{(2.425\mathrm{w} \times 90\mathrm{s})}{3600\mathrm{s}} = 0.50425\mathrm{w}$$

7.3 The cost of the concept

Table 3. Cost of different components of our concept.

Material	Unit cost ($)	Total cost ($)
The stepper motor 55SI-25DAYA	6.5	6.5
The reducer of DiseqC motor	38	38
Round and hollow tube 40cm long and 4cm thick	3	3
Two bearings UCP208	14	28
The iron structure of the equatorial mount	7	7
The iron structure of the photovoltaic panel (63×57cm)	6	6
Two mirrors added with their structure (63cm × 19.95cm × 4mm)	3	6
The control card and the solar captor	7	7
TOTAL		101.5

This cost remains reasonable by comparing it with those of other embodiments (example the cost of the prototype proposed by the publication [18]).

8. Conclusions

This paper presents a model of a mono-axial solar tracker based on the equatorial mount, in order to minimize the production and the energy consumption of the system, while keeping the efficiency of the photovoltaic panel to the maximum throughout the year. The theoretical study shows us that our solar tracker allows a yield to the photovoltaic panel, which varies between 91.7% and 100% according to the seasons compared to a surface normal to solar radiation.

As you get closer to the summer or winter solstice, the performance is minimized.

As you approach the equinoxes, the performance maximizes.

In order to compensate for the loss of yield during the solstices, we added two mirrors at the top and bottom to our photovoltaic panel with a dimension and a well-calculated angle of inclination.

After the realization, we passed to the real test in order to validate experimentally the proposed model. The results show that the proposed concept offers a gain of around 43.46% compared to a fixed system.

Perspective:

Following the experience already carried out in a single day and in order to validate and generalize the results of the new concept, We will work on the possibility of carrying out the same experiments spread over a minimum period three months, between the solstice and the equinox.

It should be noted that this model is only valid for a photovoltaic panel. Our goal is to improve it so that it will be suitable even for concentrated or high concentration photovoltaic panels.

References

[1] S. R. Wenham, M. A. Green, M. E. Watt, Richard Corkish, Applied Photovoltaics, 2nd ed., Earthscan, 2007.

[2] R. Bayindir, E. Kabalci, H. I. Bülbül, and C. Can, "Optimization of Operating Conditions of Photovoltaic Systems: A Case Study", 1st International Conference on Renewable Energy Research and Applications, Nagasaki, pp. 1-4, 11-14 November 2012.

[3] A. Ponniran, A. Hashim, and H. Ali Munir, "A Design of Single Axis Sun Tracking System", 5th International Power Engineering and Optimization Conference, Shah Alam Selangor, pp. 107-110, 6-7 June 2011.

[4] S. Ghabusnejad, A. Majdi, and S. A. Davari, "Using P&O Based Sensorless Method In SingleAxis Solar Tracker", International Journal of Renewable Energy Research, vol. 9, no 1, pp. 532-541. March, 2019. https://ijrer.org/ijrer/index.php/ijrer/article/view/8922/pdf

[5] J. Hu, and T. Yachi, "Photovoltaic Systems with Solar Tracking Mirrors", 2nd International Conference on Renewable Energy Research and Applications, Madrid, pp. 201-204, 20-23 October 2013.

[6] A. Al-Ghasem, G. Tashtoush, and M. Aladeemy, "Experimental Study of tracking 2-D Compound Parabolic Concentrator (CPC) with flat plate absorber", 2nd International Conference on Renewable Energy Research and Applications, Madrid, pp. 779-782, 20-23 October 2013.

[7] J. Beltrán A., J. L. González Rubio S., and C. D. Garcia-Beltran, "Design, Manufacturing and Performance Test of a Solar Tracker Made by a Embedded Control", Electronics, Robotics and Automotive Mechanics Conference, Morelos, pp. 129-134, 25-28 September 2007.

[8] C. Sanna, M. Garonska, and A. Damiano, "Energy Performance of Concentrator and Flat Plate Photovoltaics in the Mediterranean Area", 4th International Conference on Renewable Energy Research and Applications, Palermo, pp. 760-765, 22-25 November 2015.

[9] N. AL-Rousan, M. AL-Rousan, A. Shareiah, and H. AL-Najjar, "Choosing the Efficient Tracking Method for Real Time Tracking System in Jordan and it's neighbors to Get Maximum Gained Power Based on Experimental Data", 1st International Conference on Renewable Energy Research and Applications, Nagasaki, pp. 1-6, 11-14 November 2012.

[10] J. Kern, I. Harris, "On the optimum tilt of a solar collector", Solar Energy, DOI: 10.1016/0038-092X(75)90064-X, Vol. 17, No. 2, pp. 97-102.

[11] Z. El Jaouhari, Y. Zaz, S. Moughyt, O. El Kadmiri, Z. El Kadmiri, "Dual-axis Solar Tracker Design Based on Digital Hemispherical Imager", Journal of Solar Energy Engineering, DOI: 10.1115/1.4039098, Vol. 141, No. 1, pp. 1-8.

[12] H. M. Fahad, A. Islam, M. Islam, Md. F. Hasan, W. F. Brishty, and Md. M. Rahman, "Comparative Analysis of Dual and Single Axis Solar Tracking System Considering Cloud Cover", 2019 International Conference on Energy and Power Engineering, Dhaka, pp. 1-5, 14-16 March 2019.

[13] S. Abdallah, "The effect of using sun tracking systems on the voltage-current characteristics and power generation of flat plate photovoltaics", Energy Conversion and Management, DOI: 10.1016/j.enconman.2003.10.006, Vol. 45, No. 11-12, pp.1671-1679.

[14] S. A. Sadyrbayev, A. B. Bekbayev, S.Orynbayev, Z. Z. Kaliyev, "Design and Research of Dual-Axis Solar Tracking System in Condition of Town Almaty", Middle-East Journal of Scientific Research, DOI: 10.5829/idosi.mejsr.2013.17.12.12363, Vol. 17, No. 12, pp.1747-1751.

[15] C. Sungur, "Multi-axes sun-tracking system with PLC control for photovoltaic panels in Turkey", Renewable Energy, DOI: 10.1016/j.renene.2008.06.020, Vol. 34, No. 4, pp. 1119-1125.

[16] R. Berry, Build Your Own Telescope, 3rd ed., Willmann-Bell, 2001.

[17] M. Iqbal, An Introduction To Solar Radiation, 1st ed., Elsevier, 1983, pp.1-75.

[18] S. Gutérrez, "Prototype for an off-grid photovoltaic system with low cost solar tracking", 2017 IEEE Mexican Humanitarian Technology Conference, Puebla, pp. 7-11, 29-31 March 2017.